J Polym Res (2014) 21:358
DOI 10.1007/s10965-014-0358-y

ORIGINAL PAPER

Electrical properties of poly(arylene ether nitrile)/graphene nanocomposites prepared by in situ thermal reduction route

Zicheng Wang · Wei Yang · Xiaobo Liu

Received: 10 October 2013 / Accepted: 2 January 2014 / Published online: 18 January 2014

Abstract In order to obtain highly flexible polymer composites with high dielectric performance, novel poly(arylene ether nitrile) (PEN)/graphene nanocomposites were prepared by a two-step method, involving facile solution-casting for dispersing graphene oxide and followed by thermal reduction of dispersed graphene oxide at 200 °C for 2 h. The results showed that the in situ thermal reduction method can help to fabricate PEN-based nanocomposites with homogenously dispersed graphene sheets and give rise to a 236 % increase of the dielectric constant between 160 °C and 200 °C of from 10.43 to 24.65 at 50 Hz. As a result of the formation of an alternative multilayered structure of PEN and graphene sheets, a typical percolation transition was observed as the content of the graphene oxide increased. The conductivity and dielectric constant followed the percolation threshold power law, yielding a percolation threshold (f_c) of 0.014. The corresponding critical exponent was calculated as $\mu=t(t+s)^{-1}=0.83$, which was in good agreement with the experimental data of $\mu=0.81$ as $f_{graphene}=0.013$. This type of PEN/graphene composite with low percolation threshold can be potentially applied as novel dielectric materials.

Keywords Poly(arylene ether nitrile) · Graphene oxide · In situ thermal reduction · Dielectric · Low percolation threshold

Introduction

Poly(arylene ether nitrile) (PEN) is a well-known semicrystalline thermoplastic polymer with pendant nitrile groups. Owing to its rigid molecular structure, PEN exhibits outstanding tensile strength, good radiation resistance, high thermo-oxidative stability, and good molding workability [1–3], which make it attract considerable attention both from industry and academia. In contrast to the excellent mechanical properties and thermal stabilities, the high electrical resistivity (about 10^8 Ω m) and/or low dielectric constant (ca. 3–4) of PEN hinders its advanced applications in electrostatic and/or electromagnetic dissipation. Therefore, development of PEN composites with high dielectric constant is necessary.

A common approach for elevating the dielectric constant is to disperse high dielectric constant ceramic powders into polymer matrixes. Hence, various electrically conductive materials such as metal and carbon materials have been used to increase the dielectric constant of composites. Although the poor uniform dispersion of these conductive fillers in matrixes has been improved by physical dispersion methods such as sonication, ball milling, grinding, and high speed shearing, the effects are not fully satisfactory. Multifunctional nanoparticles, such as carbon nanotubes [4–7], graphite sheets [8–13], acetylene black [14], and carbon fiber [15], are promising conductive fillers used to obtain highly flexible polymer composites with high dielectric performance. However, to achieve sufficiently high dielectric constant, a large content of fillers is general necessary at the cost of sacrificing the excellent electrical conductivity. In addition, the high content of fillers may deteriorate the mechanical performance of the composites. Thus, the focus of the current work is how to achieve a balance the dispersion and electrical conductivity. Fortunately, in recent years, many reports have demonstrated that in situ thermal reducing graphene oxide can make it possible to address this issue.

Graphene with a two-dimensional lattice of sp^2-bonded carbon exhibits excellent electrical conductivity in the in-plane direction owing to the delocalization of the lone pair of the p_z electrons [16]. Besides, compared with other

Z. Wang · W. Yang · X. Liu (✉)
Research Branch of Functional Materials, Institute of Microelectronic & Solid State Electronic, High-Temperature Resistant Polymers and Composites Key Laboratory of Sichuan Province, University of Electronic Science and Technology of China, Chengdu 610054, People' s Republic of China
e-mail: Liuxb@uestc.edu.cn

conductive fillers, graphene possesses a large specific surface area and high aspect ratio which make it possible to form a microcapacitor in the matrixes when two graphene sheets have a compact parallel structure, isolated by a thin layer of polymer. Through forming a large microcapacitor network, the dielectric permittivity of the polymer composites can be greatly increased. However, as a result of the strong *p–p* stacking tendency and high cohesive energy, the pure graphene tends to agglomerate or restack easily [17]. In addition, the hydrophobic nature and high specific surface area of graphene make it insoluble in a variety of organic solvents. Thus, large-scale use of graphene is hindered by its poor dispersion in matrixes. In order to solve the two problems of aggregation and random distribution of graphene sheets in the composite it is necessary to use functionalization [18–21] to change the surface energy of the graphene.

At present, the most common approach to functionalize graphene is the use of strong oxidizing agents to exfoliate pristine graphite [22–25]. The previously contiguous aromatic lattice of graphene is interrupted by epoxide, hydroxy, and carboxylic groups [26, 27]. Compared with pure graphene, the hydrophilic oxygenic groups on the basal plane and edge of graphene can effectively lead to better dispersion and stronger adhesion in/to the polymer matrixes. However, graphene oxide is electrically insulating, which limits its usefulness for the preparation of conductive nanocomposites. Fortunately, the electrical conductivity of graphene oxide can be significantly increased by chemical reduction [28, 29] and thermal reduction [30–32], owing to the significant restoration of the sp^2 carbon sites.

In this paper, novel poly(arylene ether nitrile)/graphene (PEN/graphene) nanocomposites are prepared by a two-step method, involving facile solution-casting for dispersing graphene oxide and followed by in situ thermal reduction of graphene oxide dispersed in matrixes. Additionally, the dispersion, dielectric, and electrical properties of PEN/graphene nanocomposites are systematically investigated. The results indicate that the in situ thermal reduction method can effectually improve the dielectric and electrical properties of pure PEN and optimize the dispersion of graphene in PEN.

Experimental

Materials

Natural graphite was purchased from Qingdao Yanxin Graphite Co. Ltd., China. *N*-Methyl-2-pyrrolidinone (NMP), 98 % sulfuric acid (H_2SO_4), 30 % hydrogen peroxide (H_2O_2), 85 % phosphoric acid (H_3PO_4), and potassium permanganate ($KMnO_4$) were purchased from Shuanglin Chemical Reagent Factory of Hangzhou, China. All the chemicals and reagents were used without further purification. PEN was provided by Union Laboratory of Special Polymer of USETC-FEIYA, Chengdu, China. It was a copolymer derived from 2,6-dichlorobenzonitrile with hydroquinone and resorcin with an inherent viscosity of 1.22 dL/g (0.005 g/mL in NMP).

Preparation of graphene oxide

Graphene oxide (GO) was synthesized from purified natural graphite by the improved Hummers method [33]. Briefly, graphite powder (3.0 g) and a 9:1 mixture of concentrated H_2SO_4/H_3PO_4 (360/40 mL) were added into the 1,000-mL flask and stirred uniformly. Then, $KMnO_4$ (18.0 g) was gradually added with stirring and cooling in order to keep the temperature at 35–40 °C. The mixture was then stirred at 50 °C for about 12 h. The reaction was terminated by adding 30 % H_2O_2 solution (3 mL). The mixture was left overnight. Graphite oxide sheets, which settled at the bottom, were separated from the excess liquid by decantation, followed by centrifugation. Then, they was washed with a mixture aqueous solution (the volume ratio of water, H_2O_2 and H_2SO_4 is equal to 1: 0.23: 0.26) and deionized water. Graphite oxide was obtained after drying at 80 °C. Graphite oxide (500 mg) was dispersed in 500 mL water to create a yellow-brown dispersion, and the exfoliation of graphite oxide to GO was achieved by sonication with a cylindrical tip for 1 h.

Preparation and in situ thermal reduction of PEN/GO nanocomposites

A series of PEN/GO nanocomposites were generally prepared as follows. A measured quantity of GO (0, 1, 2, 3, 4, or 6 wt.%) was added to NMP under sonication for 30 min. Meanwhile, a certain content of PEN was dissolved in NMP with mechanical stirring. The mixture was continuously stirred at 160 °C for 30 min after PEN was totally dissolved. The prepared GO was then added to the PEN solution under sonication and mixed with a high-speed mechanical stirrer for 1 h. The mixture was then poured on a clean preheated glass plate and cast solvent using a sequential temperature program of 60, 80, 100, 120, 140, and 160 °C for 1 h, respectively. To ensure the effective reduction of GO, the annealing temperature was continuously increased to 200 °C for 2 h. The mixture was then cooled to room temperature gradually to afford the PEN/thermally reduced GO composite films. For comparison, a PEN/GO composite with 2 wt.% GO loading was also prepared by the same procedure as above but without annealing at 200 °C; this product was labeled S-160.

Characterizations

The morphology of GO and the fracture surfaces of the thermally reduced PEN/GO were observed by scanning electron microscopy (SEM) (JEOL JSM-5900Lv). Fourier

transform infrared spectrometry of KBr pellets (FTIR) (NICOLETMX-IE) was performed to characterize the functional groups of GO. Thermogravimetric analysis (TGA) of GO was carried out under N_2 atmosphere at a heating rate of 20 °C/min using a TA Q50 series analyzer system combined with a data processing station. Dielectric and AC conductivity measurements for the thermally reduced PEN/GO films were carried out by a dielectric analyzer (DEA 2970, TA Instruments).

Results and discussion

Thermal analysis of GO

In order to investigate the influence of heat treatment on the reaction progress of GO, TGA is used during the thermal reduction of the GO. Figure 1a shows that a dramatic mass loss of about 40 % of the original GO mass appears at the temperature range from 150 to 250 °C. This may be attributed to the loss of some oxygen-containing groups during the thermal reduction of GO. From the derivative thermogravimetric (DTG) curve, the temperature corresponding to the maximum rate of loss mass arises at 200 °C. It may demonstrate that 200 °C is a mild and efficient temperature to remove a large portion of oxygen-containing functional groups, compared with the higher annealing temperatures. Thus, the thermal reduction process of GO can be carried out at 200 °C for investigating the effect of homothermal time on the thermal reduction. As shown in Fig. 1b, the weight of GO decreases to 79.72 % by heating to 200 °C, and continues to decrease during the temperature-holding period; the final weight achieves a minimum value of 51.13 % after about 80 min. On the basis of the results in Fig. 1, heating at 200 °C for 2 h is sufficient to thermally reduce the GO.

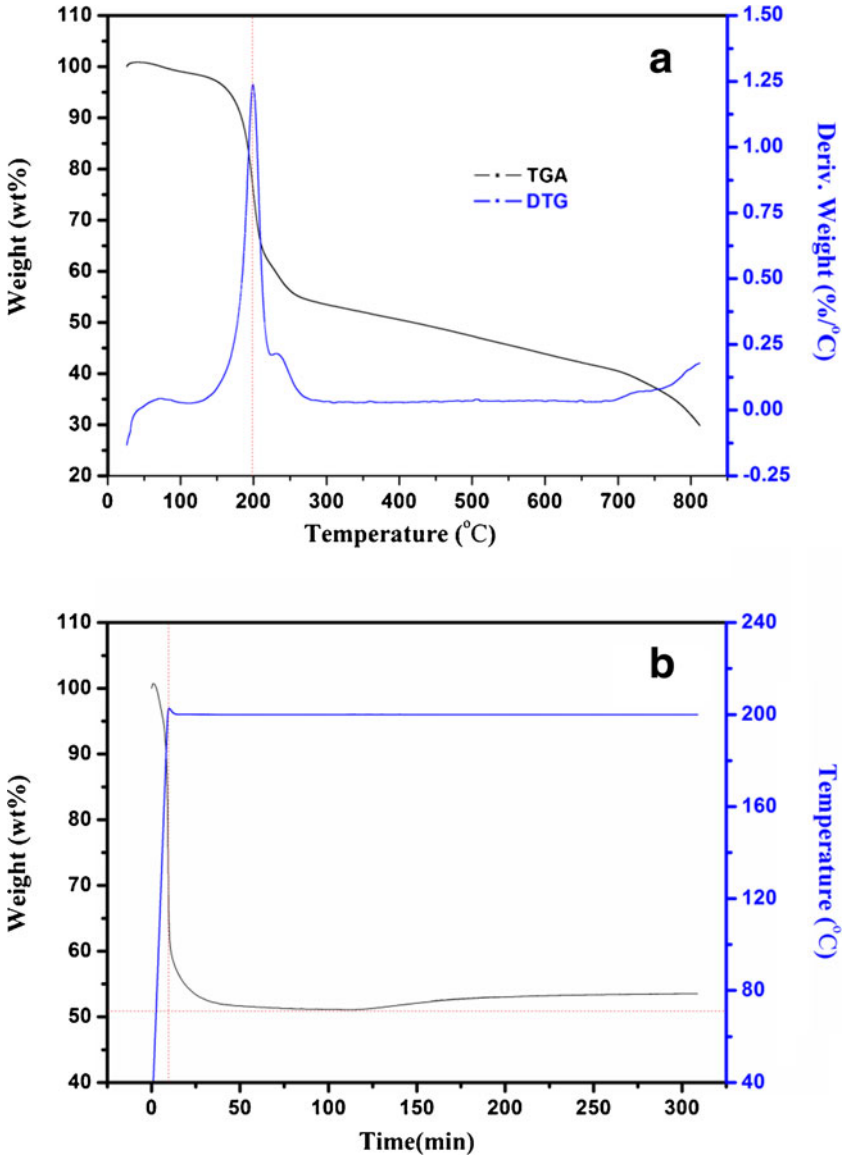

Fig. 1 Thermal analysis of graphene oxide powder: **a** TGA and DTG plot of graphene oxide and **b** the annealing process in the TGA

FTIR of GO and thermally reduced GO

To further determine the changing microstructure of the GO, the FTIR spectra of GO and thermally reduced GO at 200 °C for 2 h are shown in Fig. 2. The FTIR spectrum of GO (Fig. 2a) shows a strong peak around 1,640 cm^{-1} due to aromatic C=C, and a strong and broad absorption band at 3,430 cm^{-1} corresponding to the O–H stretching vibration. An absorption band at 1,730 cm^{-1} corresponding to the C=O stretching and the peaks corresponding to carboxy C–O (1,403 cm^{-1}), epoxy C–O (1,225 cm^{-1}), and alkoxy C–O (1,070 cm^{-1}) groups situated at the edges of GO are also observed [34]. After the GO was annealed at 200 °C for 2 h, the peaks at 3,430 and 1,730 cm^{-1} decrease significantly, the peaks at 1,403, 1,225, and 1,070 cm^{-1} disappear, and the C=C peak shifts from 1,640 to 1,569 cm^{-1}, as shown in Fig. 2b. The obvious changes of the characteristic absorption peaks indicate the breakdown between the covalent bonds of GO containing epoxide, hydroxyl, and carboxylic groups on the basal plane and edge of graphene at the annealing temperature of 200 °C after 2 h. The degradation of hydrophilic oxygenic groups suggests the thermal reduction of GO, which is consistent with the results of TGA of the sample.

Preparation of PEN/graphene nanocomposites

To optimize the thermal reduction, GO is incorporated into the PEN matrix. A typical procedure for preparing PEN/graphene via the method of in situ thermal reduction is presented in Fig. 3. The three-step process involves (1) GO preparation by means of the improved Hummers method, (2) PEN/GO nanocomposites fabrication by the method of solution casting, and (3) in situ thermal reduction of PEN/GO annealed at 200 °C for 2 h. Hence, thermally reduced GO is successfully incorporated into PEN resin.

Micromorphologies of PEN/GO and PEN/graphene nanocomposite

To evaluate the dispersion of GO in the PEN matrix, SEM is employed to investigate the morphology of the samples. As shown in Fig. 4, GO consists of thin, randomly aggregated and crumpled sheets, forming a disordered solid. The fractured surfaces of pure PEN are smooth and rarely crumpled, whereas the fractured surfaces of PEN/GO composite (S-160) are tough and crumpled as shown in Fig. 4c. And the GO sheets exhibit homogeneous dispersion in the PEN matrix without serious aggregation, which may be attributed to the existence of the hydrophilic oxygenic groups on the basal plane and edge of graphene. In addition, most GO sheets are parallel to the fracture surface, and the same is can also be observed in Fig. 4d. The thermally reduced GO sheets are homogeneously dispersed in the PEN matrix which may be attributed to that the nitrile groups on the aromatic ring appearing to promote the adhesion of the matrix and the hydrophilic oxygenic groups, and they serve as a potential site for dispersing GO. In addition, GO sheets become immobilized in the flexible polymer matrixes (PEN), when the solvent is entirely removed from the polymer matrixes after a series of annealing process. Therefore, with elevating the annealing temperature to 200 °C, the in situ thermal reduction of GO is carried out in the PEN matrixes. Heating for 2 h, partly hydrophilic oxygen groups are removed from graphene plane, hence, PEN/graphene composites are successfully prepared with a characterization of good dispersion.

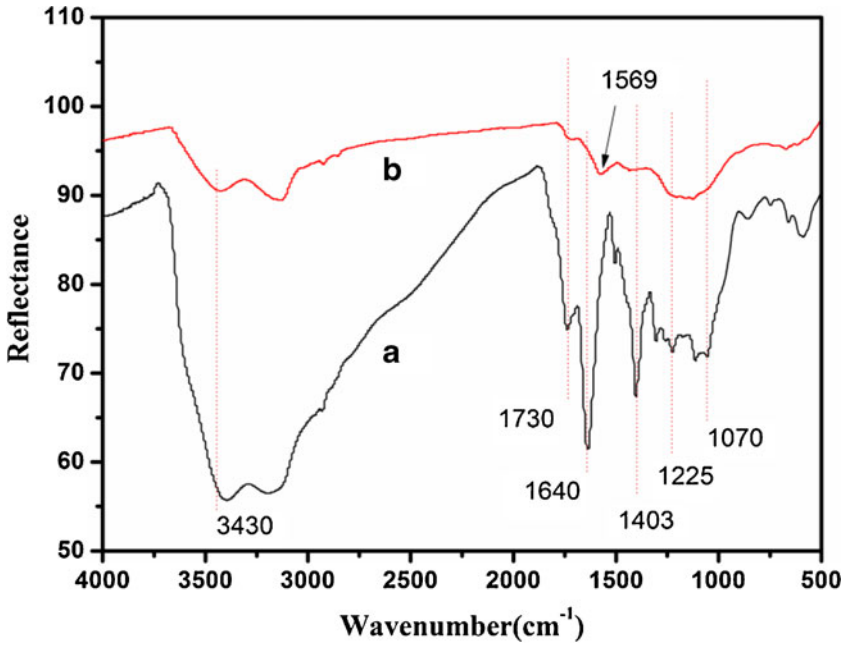

Fig. 2 FTIR spectrum of **a** graphene oxide and **b** thermally reduced graphene oxide at 200 °C for 2 h

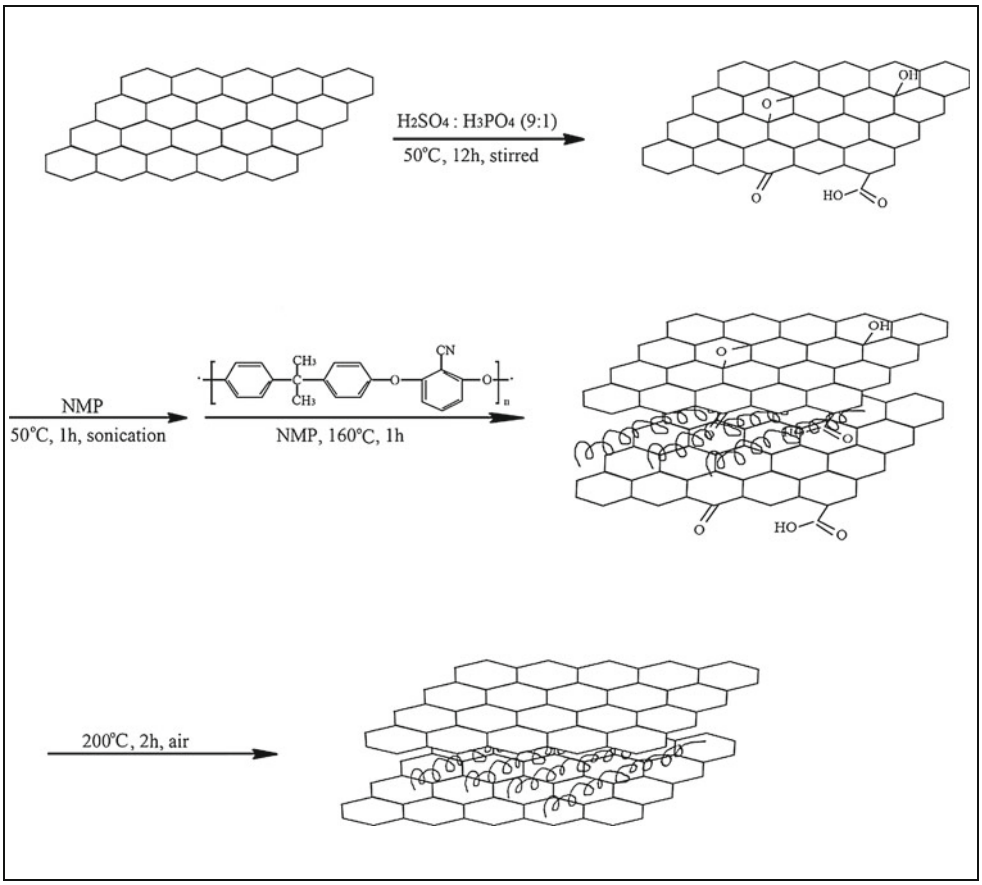

Fig. 3 Preparation of graphene oxide and PEN/graphene nanocomposites

Effect of in situ thermal reduction of GO on dielectric properties of PEN

To further investigate the effect of the in situ thermal reduction of GO on the dielectric properties of the composites, the dielectric constant and dielectric loss were monitored according to ASTM D150 using a TH2819A precision LCR meter and the results are shown in Fig. 5. It can be clearly seen that the dielectric constant and loss of pure PEN are independent of the frequency from 50 Hz to 200 kHz, whereas the dielectric constant of PEN/GO nanocomposites is dependent on annealing temperature and frequency, and shows a tendency of gradual increase with increasing annealing temperature. The dielectric constant of the sample S-160 increases from 4.86 to 10.43 at the specified frequency (50 Hz), compared with that of pure PEN. With increasing annealing temperature, a sharp increase of the dielectric constant is observed between 160 °C and 200 °C of from 10.43 to 24.65, i.e., a 236 % increase. The transitions of dielectric loss can also be observed in Fig. 5b.

The transitions of the dielectric properties of PEN/GO composites may be attributed to the large specific surface area and high aspect ratio of graphene which make it possible to form a microcapacitor structure in the matrix, isolated by a thin layer of polymer. With increasing intensity of the local electric field, the migration and accumulation of charge carriers at the interfaces between GO sheets and PEN matrix will contribute to the enhancement of dielectric properties of the PEN/GO composites at low frequency, known as Maxwell–Wagner–Sillars (MWS) interfacial polarization [35–37]. Elevating the annealing temperature to 200 °C will enhance the MWS interfacial polarization because the number of free charges in graphene will increase owing to the in situ thermal reduction of GO and restoration of the sp^2 carbon sites. And the free charges in graphene accumulate at the interface and give rise to strong MWS interfacial polarization, leading to the high increase in the dielectric constant and loss.

AC conductivity of PEN/graphene nanocomposites

The conductivity of the thermally reduced PEN/GO nanocomposites as a function of GO weight fraction was studied. Figure 6 shows the alternating current (AC) conductivity of the composites as a function of the GO weight fraction from 0.00 to 0.06, measured at room temperature and 100 Hz. As the weight fraction increases, the composites exhibit a range of conductivity values, initially behaving as an insulator, up to

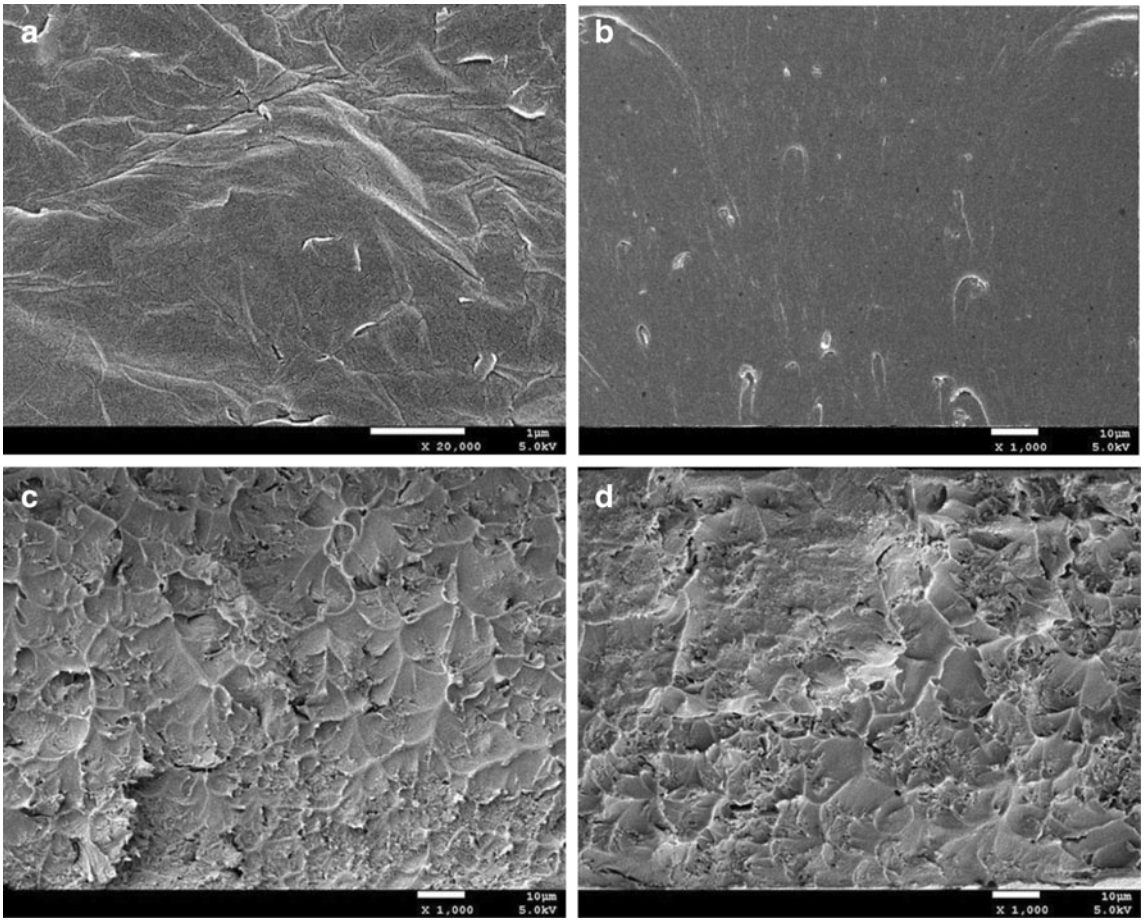

Fig. 4 SEM of graphene oxide (**a**), pure PEN (**b**), and nanocomposites with 2 wt.% graphene oxide incorporated into PEN annealed at 160 °C (**c**) and 200 °C (**d**) compared with pure PEN

approximately 10^{-4} S/m. A dramatic increase in the conductivity arises between 2 and 3 wt.%, with an increase of about 2 orders of magnitude compared to that at 2 wt.%. From that point on, the resin starts to exhibit excellent conductivity. For the composites incorporating conductive fillers, the dramatic increase in the conductivity can be explained by percolation theory according to the following:

$$\sigma_{eff} \propto \sigma_i \left(f_c - f_{graphene} \right)^{-q} \quad for \quad f_c > f_{graphene} \tag{1a}$$

$$\sigma_{eff} \propto \sigma_i \left(f_{graphene} - f_c \right)^{t} \quad for \quad f_{graphene} < f_c \,. \tag{1b}$$

where σ_{eff} is the effective conductivity of the composites, σ_{i} is the conductivity of the insulating PEN, f_{graphene} is the graphene volume fraction, f_{c} is the critical volume fraction at the percolation threshold which is a key parameter when studying the electrical properties [38, 39], q is the critical exponent in the insulating PEN, and t is the conductivity exponent. In this article, the densities of the PEN polymer and GO are 1.2 and 1.8 g/cm^3, respectively, as calculated. Thus, on the basis of the transformation from filler weight fraction to volume fraction, the best linear fit (Fig. 6b) of the conductivity data to log–log plots of the power laws for Eq. (1) gives f_{c}=0.014 and t=2.40. The critical exponent in the conducting region, t= 2.40, is larger than the universal ones (1.6–2). Similar values have also been reported for multiwall carbon nanotube (MWCNT)/polycarbonate composites [40] and graphene/PVDF composites [41]. And the t values might be related to the microstructural properties of the conductive-filler/PEN nanocomposites, such as filler size and shape [41]. The low percolation threshold is comparable to that obtained using nitrile-functionalized graphene [21] and other conductive fillers [42, 43]. This could be attributed to the high aspect ratio of the graphene and its homogeneous dispersion in the PEN matrix [44].

Dielectric properties of PEN/graphene nanocomposites

Figure 7a shows the dielectric constant of the thermally reduced PEN/GO nanocomposites as a function of the GO weight fraction. The addition of GO leads to composites with remarkably increased dielectric constant, compared with other

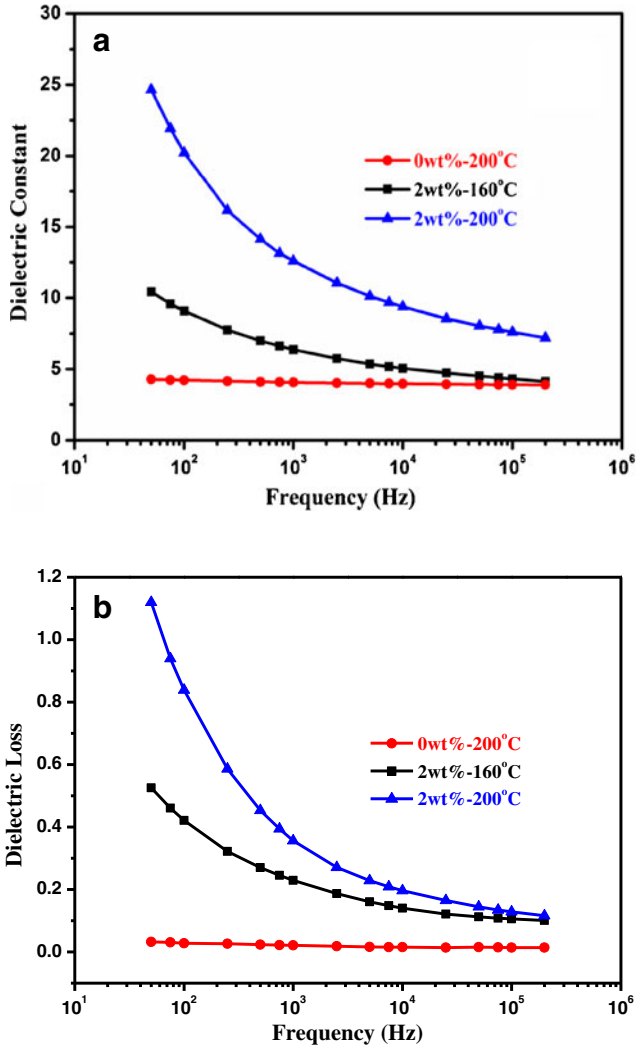

Fig. 5 Dielectric constant (**a**) and loss (**b**) curves of nanocomposites with 2 wt.% graphene oxide incorporated into PEN annealed at 160 °C and 200 °C compared with pure PEN

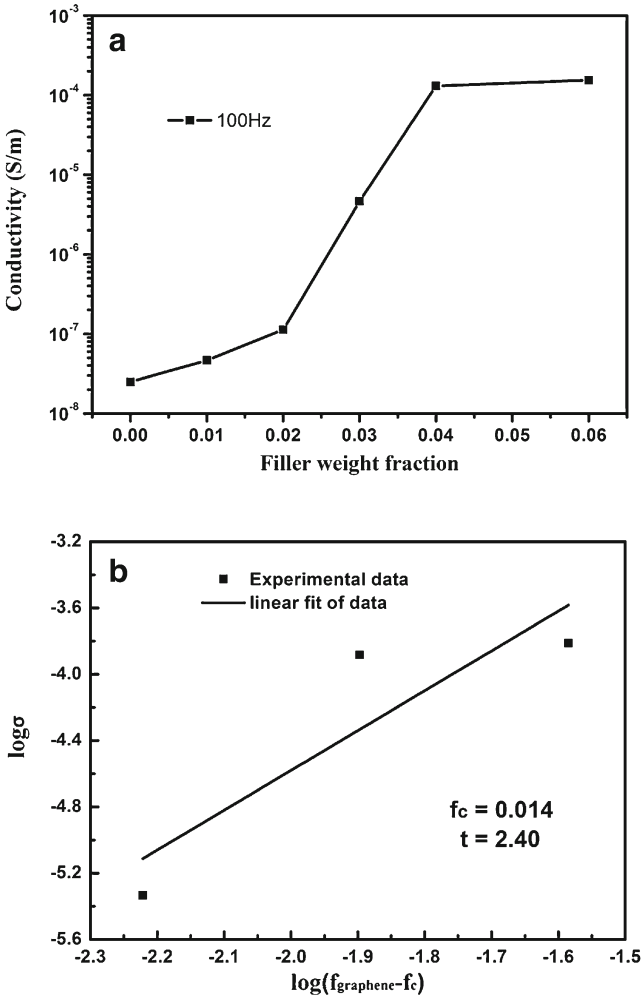

Fig. 6 **a** AC conductivity of PEN/graphene composites as a function of graphene oxide weight fraction, measured at 100Hz and room temperature. **b** Best fit of conductivity to Eq. (1)

conductive fillers [21]. The results indicate that the dielectric constant of the composite with $f_{graphene}$=0.013 (2 wt.%) is 24.65, which is about six times higher than that of pure PEN (4.86). A higher dielectric constant of 129.12 is obtained for the composite with $f_{graphene}$=0.04 (6 wt.%), which is approximately 27 times higher than the value of pure PEN. When filler content is near the percolation threshold, the dielectric constant can be expressed by the percolation theory power law in Eq. (2), as follows:

$$\varepsilon_{eff} \propto \varepsilon_i \left(f_c - f_{graphene}\right)^{-s} \quad for \quad f_{graphene} < f_c \tag{2}$$

In Eq. (2), ε_{eff} is the effective dielectric constant of the composites and s is the critical exponent. The straight line in Fig. 7b, with f_c=0.014 and s=0.49, gives a good fit to the data. And the critical exponent s is lower than the universal one (about 1) [45].

The increase of dielectric content with increasing graphene content may be ascribed to the fact that planar conductive filler graphene possesses high aspect ratios and a large surface area which make it possible to form a microcapacitor. Specifically, the conductive graphene sheets are isolated by very thin dielectric insulating-polymer layers within the matrix, forming a small number of microcapacitors, which bring about a slight increase of dielectric constant. As the graphene content increases, the homogenous, parallel, and flat dispersion of flake-like graphene in the PEN matrix can lead to a gradual formation of the microcapacitor network in the PEN/graphene nanocomposites, as shown in Fig. 7c. As a result, when the graphene content is beyond the percolation threshold, the dielectric constant is greatly increased.

Dielectric properties are also related to frequencies. Therefore, studying dielectric behaviors vs. frequency for PEN/graphene composites is necessary for their application. As shown in Fig. 8a, the dielectric constant of PEN/graphene composites demonstrates obvious dependence on the low

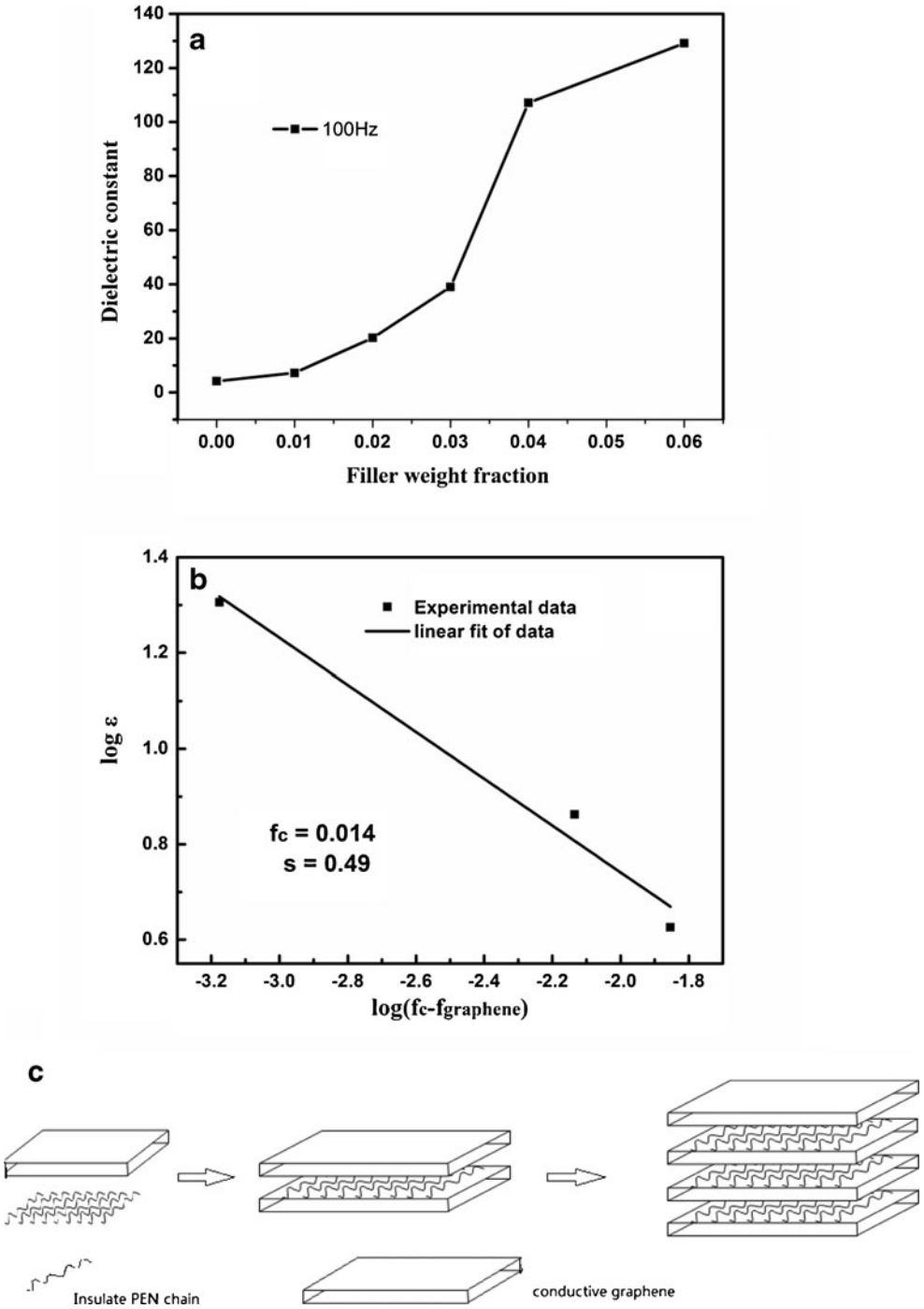

Fig. 7 **a** Dielectric constant of PEN/graphene composites as a function of graphene oxide weight fraction, measured at 100 Hz and room temperature. **b** Best fit of conductivity to Eq. (2). **c** Illustration of microcapacitor formation as graphene content increases

frequency. And the dielectric constant decreases gradually with increasing frequency at higher graphene loading. Moreover, for dielectric loss, similar results are also observed in Fig. 8b. When $f_{graphene}$ is beyond the percolation threshold, the loss shows a large and rapid increase. The behavior could be attributed to the fact that the special structure of the graphene sheets can produce an electrical current under an electrical field, bringing about the transformation of partial electrical energy into thermal energy. Meanwhile, the dielectric loss also increases with the increase of graphene.

Figure 9a displays the frequency dependence of AC conductivity (σ) of the PEN/graphene composites with different graphene content. For composites with low graphene contents ($f_{graphene}<f_c$), the conductivity plots show a strong dependence on the frequency owing to their insulating nature. The conductivity of the composites increases with increasing frequency. When the graphene loading exceeds 0.013 (2 wt.%), an insulator–semiconductor transition is clearly observed. When $f_{graphene}>f_c$, the conductivity exhibits a conducting behavior which is nearly frequency independent

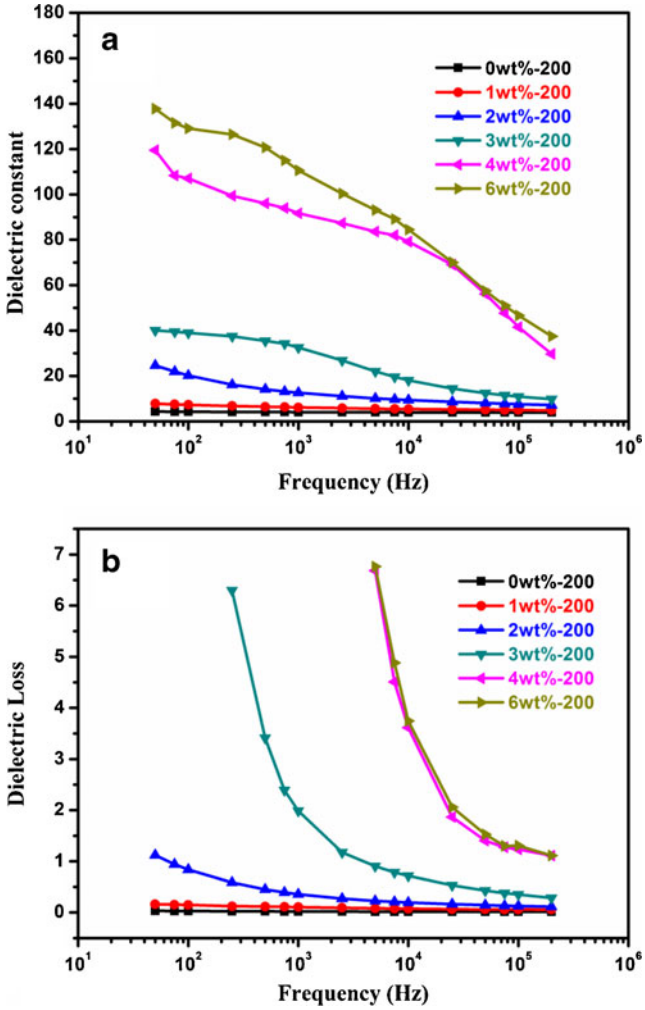

Fig. 8 Dependences of **a** dielectric constants and **b** loss tangent on frequency for the PEN/graphene composites at room temperature

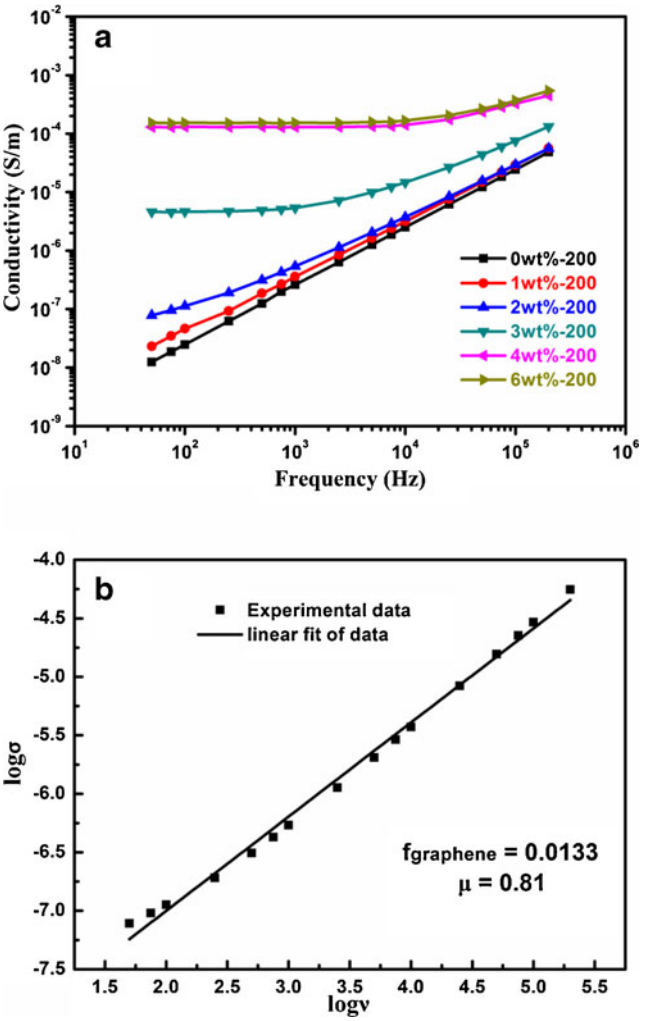

Fig. 9 Dependences of **a** AC conductivities on frequency for the PEN/graphene composites at room temperature. **b** Best fit of the effective conductivity for $f_{graphene}$=0.013 (2 wt.%) to Eq. (3)

in the frequency range of 10^1–10^7 Hz. The results are in good agreement with the variation of dielectric properties of the PEN/graphene nanocomposites. When the graphene content approaches f_c, the percolation threshold power law is described as

$$\sigma \propto \omega^{\mu} \quad as \quad f_{graphene} \rightarrow f \tag{3}$$

In Eq. (3), $\omega=2\pi\upsilon$, where υ is the frequency, and μ is the corresponding critical exponent. As shown in Fig. 9b, the experimental data for the composites with $f_{graphene}$=0.013 (2 wt.%) give μ=0.81, which is slightly smaller than the following calculated value:

$$\mu = t(t+s)^{-1} = 2.40(2.40+0.49)^{-1} = 0.83.$$

This discrepancy may be attributed to the dimensional singularity of the graphene and the deviation between $f_{graphene}$=0.013 (2 wt.%) and percolation threshold f_c=0.014.

Conclusion

Novel poly(arylene ether nitrile)/graphene nanocomposites were successfully prepared by a two-step method, involving facile solution-casting for dispersing graphene oxide and followed by thermal reduction of dispersed graphene oxide at 200 °C for 2 h. The results show that the in situ thermal reduction method can help to fabricate nanocomposites with graphene sheets homogenously dispersed in the PEN matrix and give rise to a 236 % increase of the dielectric constant between 160 °C and 200 °C of from 10.43 to 24.65 at 50 Hz. As a result of the formation of an alternative multilayered structure of PEN and graphene sheets, a typical percolation transition was observed as the content of the graphene oxide increased. Near the low percolation threshold, the conductivity showed a dramatic increase as high as 2 orders of magnitude. Moreover, a large dielectric constant of 24.65 at 50 Hz could be obtained within the vicinity of the percolation

threshold in the sample with $f_{graphene}$=0.013 and it is six times higher than that of pure PEN. The conductivity and dielectric constant followed the percolation threshold power law, yielding a low percolation threshold (f_c) of 0.014. The corresponding critical exponent was calculated as $\mu=t(t+s)^{-1}=0.83$, which agreed well with the experimental data of μ=0.81 as $f_{graphene}$=0.013. This type of PEN/graphene composite with low percolation threshold can be potentially applied as a novel dielectric material.

Acknowledgments The authors wish to thank the National Natural Science Foundation (No. 51173021) and "863" National Major Program of High Technology (2012AA03A212) for financial support of this work.

References

1. Saxena A, Sadhana R, Rao VL, Kanakavel M, Ninan KN (2003) Polym Bull 50:219–226
2. Saxena A, Rao VL, Ninan KN (2003) Eur Polym J 39:401–405
3. Matsuo S, Murakami T, Takasawa RJ (1993) Polym Sci Polym Chem 31:3439–3446
4. Ajayan PM, Schadler LS, Giannaris C, Rubio A (2000) Adv Mater 12:750–753
5. Thostenson ET, Ren Z, Chou TW (2001) Comput Sci Technol 61: 1899–1912
6. Liu XB, Long SR, Luo DW, Chen WJ, Cao GP (2008) Mater Lett 62: 19–22
7. Guo H, Sreekumar TV, Liu T, Minus M, Kumar S (2005) Polymer 46:3001–3005
8. Ezquerra TA, Kulescza M, Balta-Calleja FJ (1991) Synth Met 41: 915–920
9. Saunders DS, Galea SC, Deirmendjian GK (1993) Composite 24: 309–321
10. Stankovich S, Dikin DA, Dommett GHB, Kohlhaas KM, Zimney EJ, Stach EA, Piner RD, Nguyen ST, Ruoff RS (2006) Nature 442:282–286
11. Wakabayashi K, Pierre C, Dikin DA, Ruoff RS, Ramanathan T, Brinson LC, Torkelson JM (2008) Macromolecules 41:1905–1908
12. Zhan YQ, Lei YJ, Meng FB, Zhong JC, Zhao R, Liu XB (2011) J Mater Sci 46:824–831
13. Chen GH, Weng WG, Wu DJ, Wu CL, Lu JR, Wang PP, Chen XF (2004) Carbon 42:753–759
14. Chen Q, Du PY, Jin L, Weng WJ, Han GR (2007) Appl Phys Lett 91: 022912
15. Dang ZM, Wu JP, Xu HP, Yao SH, Jiang MJ, Bai JB (2007) Appl Phys Lett 91:072912
16. Garcia AG, Baltazar SE, Castro AHR, Robles JFP, Rubio A (2008) J Comput Theor Nanosci 5:1–9
17. Li D, Muller MB, Gilje S, Kaner RB, Wallace GG (2008) Nat Nanotechnol 3:101–105
18. Fang M, Wang KG, Lu HB, Yang YL, Nutt S (2010) J Mater Chem 20:1982–1992
19. Yang JT, Wu MJ, Chen F, Fei ZD, Zhong MQ (2011) J Supercrit Fluid 56:201–207
20. Yang HF, Shan CS, Li FH, Han DX, Zhang QX, Niu L (2009) Chem Commun 26:3880–3882
21. Yang XL, Zhan YQ, Yang J, Tang HL, Meng FB, Zhong JC, Zhao R, Liu XB (2012) Polym Int 61:880–887
22. Higginbotham AL, Lomeda JR, Morgan AB, Tour JM (2009) Appl Mater Interfaces 1:2256–2261
23. Hummers WS, Offeman RE (1958) J Am Chem Soc 80:1339–1339
24. Lerf A, He H, Forster M, Klinowski J (1998) J Phys Chem B 102: 4477–4482
25. Dreyer DR, Park S, Bielawski CW, Ruoff R (2010) Chem Soc Rev 39:228–240
26. Uhl F, Wilkie C (2004) Polym Degrad Stab 84:215–226
27. Stankovich S, Piner R, Chen X, Wu N, Nguyen S, Ruoff R (2006) J Mater Chem 16:155–158
28. Vaia RA, Wagner HD (2004) Mater Today 7:32–37
29. Du XS, Xiao M, Meng YZ (2004) Synth Met 143:129–132
30. Zhu YW, Stoller MD, Cai WW, Velamakanni A, Piner RD, Chen D, Ruoff RS (2011) ACS Nano 4:1227–1233
31. Gao XF, Jang J, Nagase S (2010) J Phys Chem C 114:832–842
32. Chen WF, Yan LF, Prakriti RB (2010) Carbon 48:1146–1152
33. Marcano DC, Kosynkin DV, Berlin JM, Sinitskii A, Sun Z, Slesarev A, Alemany LB, Lu W, Tour JM (2010) ACS Nano 4:4806–4816
34. Zhu CZ, Guo SJ, Fang YX, Dong SJ (2010) ACS Nano 4:2429–2437
35. Dang ZM, Wang L, Yin Y, Zhang Q, Lei QQ (2007) Adv Mater 19: 852–857
36. He F, Lau S, Chan HL, Fan JT (2009) Adv Mater 21:710–715
37. Wang DR, Zhang XM, Zha JW, Zhao J, Dang ZM, Hu GH (2013) Polymer 54:1916–1922
38. Xu H, Cheng ZY, Olson D, Mai T, Zhang QM (2001) Appl Phys Lett 78:2360
39. Song Y, Noh TW, Lee SI, Gaines JR (1986) Phys Rev B 33:904–908
40. Pötschke P, Abdel-Goad M, Alig I, Dudkin S, Lellinger D (2004) Polymer 45:8863–8870
41. Fan P, Wang L, Yang JT, Chen F, Zhong MQ (2012) Nanotechnology 23:365702
42. Li C, Gu Y, Liu XB, Zou YB, Tang AB (2006) Thin Solid Films 515: 1872
43. Zhong JC, Tang HL, Chen YW, Liu XB (2010) J Mater Sci Mater Electron 21:1244–1248
44. Garboczi EJ, Snyder KA, Douglas JF, Thorpe MF (1995) Phys Rev E 52:819–828
45. Nan CW (1993) Prog Mater Sci 37:1–116